Flavor content of nucleon form factors in the space- and time-like region

Roelof Bijker[a] *

[a]ICN-UNAM, AP 70-543, 04510 México DF, México

I discuss a two-component model of nucleon form factors in which the external photon couples both to an intrinsic three-quark structure and to a meson cloud via vector-meson dominance, and present a simultaneous analysis of the electromagnetic form factors of the nucleon in the space- and time-like regions as well as their strangeness content.

1. INTRODUCTION

The structure of the nucleon is of fundamental importance in nuclear and particle physics [1]. It has been investigated for many decades, from the measurement of the anomalous magnetic moment of the nucleon in the 1930's [2], the radius in the 1950's [3], to the discovery of point-like constituents in the 1960's [4].

Recent experimental data on electromagnetic form factors, such as the momentum dependence of the ratio of electric and magnetic form factors of the proton from polarization transfer experiments [5, 6], the strange form factors of the proton from parity-violating electron scattering (PVES) experiments [7] and the ratio of electric to magnetic form factors in the time-like region from electron-positron annihilation experiments [8], have provided new and unexpected insights into the structure of the nucleon and the underlying dynamics of nonperturbative QCD.

The aim of this contribution is to present a simultaneous analysis of the electromagnetic form factors of the nucleon in the space- and time-like regions as well as their strangeness content.

2. NUCLEON FORM FACTORS

Electromagnetic form factors are key ingredients in the understanding of the internal structure of composite particles like the nucleon since they contain the information about the distribution of electric charge and magnetization. The electric and magnetic form factors, G_E and G_M, are obtained from the Dirac and Pauli form factors, F_1 and F_2, by the relations $G_E = F_1 - \tau F_2$ and $G_M = F_1 + F_2$ with $\tau = Q^2/4M_N^2$.

The recent polarization transfer data for the proton form factor ratio are in excellent agreement with the predictions of a two-component model of the nucleon [9] in which the external photon couples both to an intrinsic structure and to the intermediate vector mesons (ρ, ω, ϕ) via vector-meson dominance (VMD). In its original version, the Dirac form factor was attributed to both the intrinsic structure and the meson cloud, and the

*Supported in part by a grant from CONACyT, Mexico

Pauli form factor entirely to the meson cloud. In a modified version [10], it was shown that the addition of an intrinsic part to the isovector Pauli form factor as suggested by studies of relativistic constituent quark models in the light-front approach [11], improves the results for the elecromagnetic form factors of the neutron considerably.

In order to incorporate the contribution of the isocalar (ω and ϕ) and isovector (ρ) vector mesons, it is convenient to introduce isoscalar and isovector Dirac and Pauli form factors. The isoscalar form factors contain the couplings to the ω and ϕ mesons [9]

$$\begin{aligned} F_1^{I=0}(Q^2) &= \frac{1}{2} g(Q^2) \left[1 - \beta_\omega - \beta_\phi + \beta_\omega \frac{m_\omega^2}{m_\omega^2 + Q^2} + \beta_\phi \frac{m_\phi^2}{m_\phi^2 + Q^2} \right], \\ F_2^{I=0}(Q^2) &= \frac{1}{2} g(Q^2) \left[\alpha_\omega \frac{m_\omega^2}{m_\omega^2 + Q^2} + \alpha_\phi \frac{m_\phi^2}{m_\phi^2 + Q^2} \right], \end{aligned} \tag{1}$$

and the isovector ones the couplings to the ρ meson [10]

$$\begin{aligned} F_1^{I=1}(Q^2) &= \frac{1}{2} g(Q^2) \left[1 - \beta_\rho + \beta_\rho \frac{m_\rho^2}{m_\rho^2 + Q^2} \right], \\ F_2^{I=1}(Q^2) &= \frac{1}{2} g(Q^2) \left[\frac{\mu_p - \mu_n - 1 - \alpha_\rho}{1 + \gamma Q^2} + \alpha_\rho \frac{m_\rho^2}{m_\rho^2 + Q^2} \right]. \end{aligned} \tag{2}$$

This parametrization ensures that the three-quark contribution to the anomalous magnetic moment is purely isovector, as given by $SU(6)$. The intrinsic form factor is a dipole $g(Q^2) = (1 + \gamma Q^2)^{-2}$ which coincides with the form used in an algebraic treatment of the intrinsic three-quark structure [12]. The large width of the ρ meson which is crucial for the small Q^2 behavior of the form factors, is taken into account in the same way as in [9, 10]. For small values of Q^2 the form factors are dominated by the meson dynamics, whereas for large values they satisfy the asymptotic behavior of p-QCD, $F_1 \sim 1/Q^4$ and $F_2 \sim 1/Q^6$ [13].

3. FLAVOR CONTENT

The flavor content of the electromagnetic form factors of the nucleon can be studied by combining the nucleon's response to the electromagnetic and weak neutral vector currents [14]. The strange quark content is of special interest because it provides a direct probe of the quark-antiquark sea. It can be determined assuming charge symmetry and combining parity-violating asymmetries with measurements of the electric and magnetic form factors of the proton and neutron [15, 16].

In VMD models, the strangeness content of the nucleon form factors arises through the coupling of the strange current to the isocalar vector mesons ω and ϕ [17]. Under the assumption that the momentum dependence of the strange form factors is the same as that of the isoscalar ones, the strange Dirac and Pauli form factors are expressed as [18]

$$\begin{aligned} F_1^s(Q^2) &= \frac{1}{2} g(Q^2) \left[\beta_\omega^s \frac{m_\omega^2}{m_\omega^2 + Q^2} + \beta_\phi^s \frac{m_\phi^2}{m_\phi^2 + Q^2} \right], \\ F_2^s(Q^2) &= \frac{1}{2} g(Q^2) \left[\alpha_\omega^s \frac{m_\omega^2}{m_\omega^2 + Q^2} + \alpha_\phi^s \frac{m_\phi^2}{m_\phi^2 + Q^2} \right]. \end{aligned} \tag{3}$$

The isocalar and strange couplings appearing in Eqs. (1) and (3) depend on the same nucleon-meson and current-meson couplings [17] and are constrained by the electric charges and magnetic moments of the nucleon

$$\beta^s_\omega/\beta_\omega = \alpha^s_\omega/\alpha_\omega = -\sqrt{6}\,\sin\epsilon/\sin(\theta_0+\epsilon)\ , \qquad \alpha_\omega = \mu_p+\mu_n-1-\alpha_\phi\ ,$$
$$\beta^s_\phi/\beta_\phi = \alpha^s_\phi/\alpha_\phi = -\sqrt{6}\,\cos\epsilon/\cos(\theta_0+\epsilon)\ , \qquad \beta_\phi = -\beta_\omega\tan\epsilon/\tan(\theta_0+\epsilon)\ , \qquad (4)$$

with $\tan\theta_0 = 1/\sqrt{2}$. The angle ϵ represents the deviation from the ideally mixed states $|\omega_0\rangle = (u\bar{u}+d\bar{d})/\sqrt{2}$ and $|\phi_0\rangle = s\bar{s}$. Here we use the value $\epsilon = 0.053$ rad (or 3.0°) which was determined from the radiative decays of the ω and ϕ mesons [19].

4. RESULTS

4.1. Space-like form factors

In order to calculate the nucleon form factors in the two-component model, the five remaining coefficients, γ from the intrinsic form factor, the isoscalar couplings β_ω and α_ϕ, and the isovector couplings β_ρ and α_ρ, are determined in a least-square fit to the electric and magnetic form factors of the nucleon [10, 18].

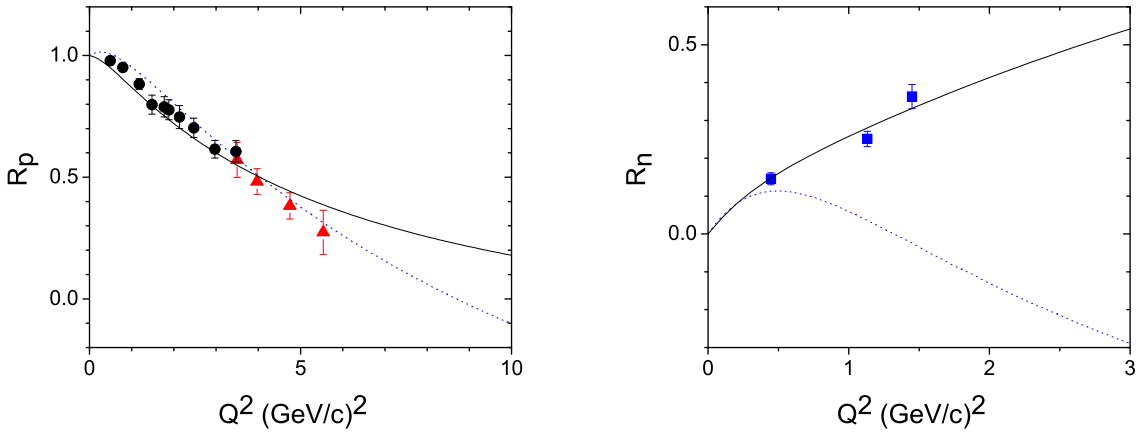

Figure 1. Comparison between the experimental and theoretical form factor ratios $R_p = \mu_p G_{E_p}/G_{M_p}$ (left) and $R_n = \mu_n G_{E_n}/G_{M_n}$ (right). The experimental data are taken from [5] (circles), [6] (triangles) and [20] (squares). The solid line represents the present calculation and the dotted line [9].

Fig. 1 shows the form factors ratios for the proton and neutron. The linear drop in the proton form factor ratio was predicted as early as 1973 in a VMD model [9] (dotted line) and later also in a chiral soliton model [21]. The experimental data for the neutron form factor ratio [20] are in agreement with [9] for small values of Q^2, but not so for

higher values of Q^2. The present calculation (solid line) is in good agreement with the data, especially for the neutron.

4.2. Strange form factors

The strange form factors are obtained by combining Eqs. (3) and (4) with the fitted values of β_ω and α_ϕ [18, 22]. Figure 2 shows the strange electric and magnetic form factors as a function of Q^2. The qualitative features of these form factors can be understood easily in the limit of ideally mixed mesons, *i.e.* zero mixing angle $\epsilon = 0°$ (in comparison with the value of $\epsilon = 3.0°$ used in the present calculations). In this limit, the Dirac form factor vanishes identically and the Pauli form factor only depends on the tensor coupling α_ϕ^s. Therefore, the strange magnetic form factor $G_M^s = F_2^s$ drops as $1/Q^6$ and has the same sign as α_ϕ^s (positive), whereas for small values of Q^2 the strange electric form factor $G_E^s = -\tau F_2^s$ is suppressed by $\tau = Q^2/4M_N^2$.

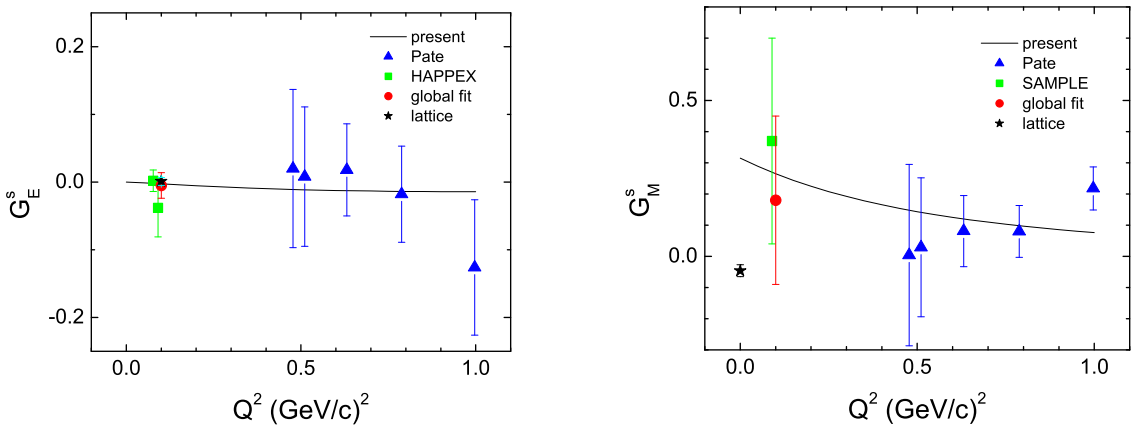

Figure 2. Comparison between theoretical and experimental values of the strange electric (left) and magnetic (right) form factor. The experimental values are taken from [23, 24, 25] (squares), [24] (circles) and [26] (triangles). The lattice results are taken from [27] (stars).

The theoretical values for G_E^s are small and negative, in agreement with the experimental results of the HAPPEX Collaboration in which G_E^s was determined in PVES from ^{4}He [23, 24]. The values of G_M^s are positive, since they dominated by the contribution from the Pauli form factor. The sign and magnitude are in agreement with the experimental result from SAMPLE [25]. A global fit of all measurements at $Q^2 = 0.1$ (GeV/c)^2 gives $G_M^s = 0.18 \pm 0.27$ [24]. The other experimental values of G_E^s and G_M^s in Fig. 2 for $0.4 < Q^2 < 1.0$ (GeV/c)^2 were obtained [26] by combining the (anti)neutrino scattering data [28] with the parity-violating asymmetries [7, 29]. The strange magnetic moment is calculated to be $\mu_s = 0.315\ \mu_N$, whose sign is in contradiction with most theoretical calculations [15, 16], but in agreement with the available experimental data [24, 25, 30].

Recent lattice calculations of the strange magnetic moment give a small negative value $\mu_s = -0.046 \pm 0.019\ \mu_N$ [27].

Most available data on strange form factors are for linear combinations of electric and magnetic form factors $G_E^s + \eta G_M^s$ [7, 24, 29, 30, 31]. An analysis of these data shows a good overall agreement with the theoretical values of the two-component model [18, 22].

4.3. Time-like form factors

For a global understanding of the structure of the nucleon it is important to study the nucleon form factors in the time-like region as well [32, 33, 34]. Whereas in the space-like (SL) region ($Q^2 > 0$) the electromagnetic form factors can be studied through electron scattering, in the time-like (TL) region ($q^2 = -Q^2 > 0$) they can be measured through the creation or annihilation of a nucleon-antinucleon pair. SL nucleon form factors are real because of the hermiticity of the electromagnetic interaction, while TL form factors are complex. Theoretically, they are related by analytic continuation $Q^2 = -q^2 \to q^2 \exp(-i\pi)$: $F^{(SL)}(Q^2) \to F^{(TL)}(q^2)$. The analytic structure of the form factors leads to a rigorous prescription of their asymptotic behavior via the Phragmèn-Lindelöf theorem [35]

$$\lim_{Q^2\to\infty} F^{(SL)}(Q^2) = \lim_{q^2\to\infty} F^{(TL)}(q^2), \tag{5}$$

implying that in the asymptotic limit the imaginary part of the TL form factors vanishes, whereas the real parts of the TL and SL form factors coincide. In previous studies of TL form factors in the two-component model [10, 36] a phase was added to the intrinsic part in order to move the singularity at $q^2 = 1/\gamma$ from the real axis. This extra phase has however the disadvantage that the Phragmèn-Lindelöf theorem is no longer satisfied [35].

Fig. 3 shows that the present calculation agrees with the recent BABAR data [8] close to threshold ($q^2 = 4M_N^2$) and for large values of q^2, but shows serious discrepancies for intermediate values. At the moment, the available experimental information does not allow to separate the contributions from the electric and magnetic form factors, nor to measure their relative phase. In the extraction of $|G_{M_p}|$ from the data it was assumed that $|G_{E_p}| = |G_{M_p}|$ which is true at threshold, but not in general.

Polarization observables are sensitive probes of different models of the nucleon, as can be seen in the second panel of Fig. 3 which shows a comparison of different theoretical predictions for $P_y \propto \mathrm{Im}(G_E^* G_M)$. The present calculation is the only one for which P_y vanishes in the asymptotic region, as required by the Phragmèn-Lindelöf theorem.

5. SUMMARY AND CONCLUSIONS

In this contribution, I presented the results of a simultaneous study of the nucleon form factors in the space- and time-like regions as well as their strangeness content. The analysis was carried out in a VMD approach in which the two-component model of Bijker and Iachello for the electromagnetic nucleon form factors [10] is combined with the method proposed by Jaffe to determine the strangeness content via the coupling of the strange current to the ϕ and ω mesons [17]. The strange couplings are completely fixed by the electromagnetic form factors of the proton and neutron.

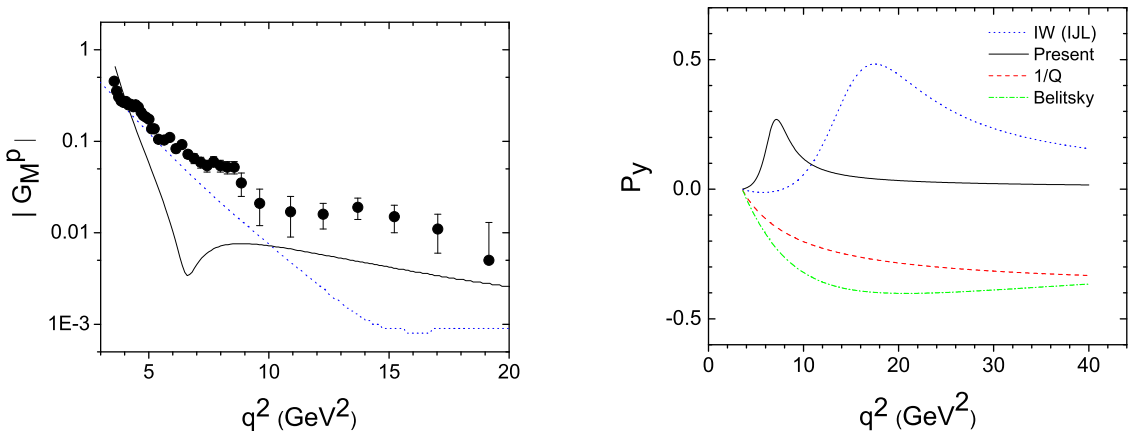

Figure 3. (left) Comparison between theoretical and experimental values of the time-like proton magnetic form factor $|G_{M_p}|$. The experimental values are taken from [8] under the assumption $|G_{E_p}| = |G_{M_p}|$. The solid line represents the present calculation and the dotted line [36]. (right) Comparison of different predictions for P_y. The solid line represents the present calculation, and the others are taken from [37].

A comparison with the available experimental data on the space-like form factors and their strange quark content shows that the present approach provides a simultaneous and consistent description of the electromagnetic and weak vector form factors of the nucleon. The strangeness contribution to the charge and magnetization distributions is of the order of a few percent [22]. Future experiments on PVES to backward angles and neutrino scattering will make it possible to determine the contributions of the different quark flavors to the electric, magnetic and axial form factors, and thus to gain new insights into the complex structure of the nucleon.

However, in the time-like region there are some serious discrepancies. The present results point once again to the inconsistency between space-like and time-like data already noted in [10, 32, 36]. In the extraction of the experimental values of the proton magnetic form factor it is assumed that $|G_{E_p}| = |G_{M_p}|$ which is true at threshold, but not for $q^2 > 4M_N^2$. For the neutron, the electric form factor is assumed to be zero $|G_{E_n}| = 0$. A remeasurement of the time-like data in which the contributions of the electric and magnetic form factors are separated, as well as a measurement of the polarization observables and a determination of the relative phase of electric and magnetic form factors may help to resolve this inconsistency.

REFERENCES

1. A.W. Thomas and W. Weise, *The Structure of the Nucleon*, (Wiley-VCH, Berlin, 2001).
2. I. Estermann, R. Frisch and O. Stern, Nature **132** (1933) 169.

3. R. Hofstadter, Annu. Rev. Nucl. Sci. **7** (1957) 231.
4. J.I. Friedman and H.W. Kendall, Annu. Rev. Nucl. Sci. **22** (1972) 203.
5. M.K. Jones *et al.*, Phys. Rev. Lett. **84** (2000) 1398;
   V. Punjabi *et al.*, Phys. Rev. C **71** (2005) 055202.
6. O. Gayou *et al.*, Phys. Rev. Lett. **88** (2002) 092391.
7. D.S. Armstrong *et al.*, Phys. Rev. Lett. **95** (2005) 092001.
8. B. Aubert *et al.*, Phys. Rev. D **73** (2006) 012005.
9. F. Iachello, A.D. Jackson and A. Lande, Phys. Lett. B **43** (1973) 191.
10. R. Bijker and F. Iachello, Phys. Rev. C **69** (2004) 068201;
    R. Bijker, Rev. Mex. Fís. S **52** (2006) 17 [arXiv:nucl-th/0502050].
11. M.R. Frank, B.K. Jennings and G.A. Miller, Phys. Rev. C **54** (1996) 920;
    E. Pace, G. Salmè, F. Cardarelli and S. Simula, Nucl. Phys. A **666** (2000) 33c.
12. R. Bijker, F. Iachello and A. Leviatan, Ann. Phys. (N.Y.) **236** (1994) 69.
13. G.P. Lepage and S.J. Brodsky, Phys. Rev. Lett. **43** (1979) 545;
    G.P. Lepage and S.J. Brodsky, Phys. Rev. D **22** (1980) 2157.
14. D.B. Kaplan and A. Manohar, Nucl. Phys. B **310** (1988) 527;
    R.D. McKeown, Phys. Lett. B **219** (1989) 140;
    D.H. Beck, Phys. Rev. D **39** (1989) 3248.
15. D.H. Beck and R.D. McKeown, Annu. Rev. Nucl. Part. Sci. **51** (2001) 189.
16. D.H. Beck and B.R. Holstein, Int. J. Mod. Phys. E **10** (2001) 1.
17. R.L. Jaffe, Phys. Lett. B **229** (1989) 275.
18. R. Bijker, J. Phys. G: Nucl. Part. Phys. **32** (2006) L49 [arXiv:nucl-th/0511060].
19. P. Jain *et al.*, Phys. Rev. D **37** (1988) 3252.
20. R. Madey *et al.*, Phys. Rev. Lett. **91** (2003) 122002.
21. G. Holzwarth, Z. Phys. A **356** (1996) 339.
22. R. Bijker, arXiv:nucl-th/0607058.
23. K.A. Aniol *et al.*, Phys. Rev. Lett. **96** (2006) 022003.
24. A. Acha *et al.*, arXiv:nucl-ex/0609002.
25. D.T. Spayde *et al.*, Phys. Lett. B **583** (2004) 79;
    E.J. Beise, M.L. Pitt and D.T. Spayde, Prog. Part. Nucl. Phys. **54** (2005) 289.
26. S.F. Pate, Phys. Rev. Lett. **92** (2004) 082002;
    S.F. Pate *et al.*, arXiv:hep-ex/0512032.
27. D.B. Leinweber *et al.*, Phys. Rev. Lett. **94** (2005) 212001;
    D.B. Leinweber *et al.*, Phys. Rev. Lett. **97** (2006) 022001.
28. L.A. Ahrens *et al.*, Phys. Rev. D **35** (1987) 785.
29. K.A. Aniol *et al.*, Phys. Rev. C **69** (2004) 065501.
30. K.A. Aniol *et al.*, Phys. Lett. B **635** (2006) 275.
31. F.E. Maas *et al.*, Phys. Rev. Lett. **93** (2004) 022002;
    F.E. Maas *et al.*, Phys. Rev. Lett. **94** (2005) 152001.
32. H.-W. Hammer, U.-G. Meissner and D. Drechsel, Phys. Lett. B **385** (1996) 343.
33. S. Dubnička *et al.*, J. Phys. G: Nucl. Part. Phys. **29** (2003) 405.
34. E. Tomasi-Gustafsson *et al.*, Eur. Phys. J. A **24** (2005) 419.
35. E. Tomasi-Gustafsson and G.I. Gakh, Eur. Phys. J. A **26** (2005) 285.
36. F. Iachello and Q. Wan, Phys. Rev. C **69** (2004) 055204.
37. S.J. Brodsky *et al.*, Phys. Rev. D **69** (2004) 054022.